

Thickness and strain effects on electronic structures of transition metal dichalcogenides: 2H-MX_2 semiconductors ($M = \text{Mo, W}$; $X = \text{S, Se, Te}$)

Won Seok Yun,^{1,2} S. W. Han,^{1,*} Soon Cheol Hong,^{1,†} In Gee Kim,² and J. D. Lee³

¹*Department of Physics and Energy Harvest-Storage Research Center, University of Ulsan, Ulsan 680-749, Republic of Korea*

²*Graduate Institute of Ferrous Technology, Pohang University of Science and Technology, Pohang 790-784, Republic of Korea*

³*School of Materials Science & Research Center for Integrated Science, Japan Advanced Institute of Science and Technology, Ishikawa 923-1292, Japan*

(Received 21 November 2011; published 17 January 2012)

Using the first-principles calculations, we explore the electronic structures of 2H-MX_2 ($M = \text{Mo, W}$; $X = \text{S, Se, Te}$). When the number of layers reduces to a single layer, the indirect gap of bulk becomes a direct gap with larger gap and the band curvatures are found to lead to the drastic changes of effective masses. On the other hand, when the strain is applied on the single layer, the direct gap becomes an indirect gap and the effective masses vary. Especially, the tensile strain reduces the gap energy and effective masses while the compressive strain enhances them. Furthermore, the much larger tensile stress leads to become metallic.

DOI: [10.1103/PhysRevB.85.033305](https://doi.org/10.1103/PhysRevB.85.033305)

PACS number(s): 31.15.A-, 71.20.Mq, 73.30.+y

The trigonal-prismatic transition metal dichalcogenides (TMDs)¹ are quasi-two-dimensional, highly anisotropic-layered compounds that are of great interest in basic research due to a large variety of electronic behaviors such as semiconductivity, superconductivity, or charge density wave, as well as in applications in areas such as lubrication, catalysis, electrochemical photocells, and battery systems. TMDs generally have two types of MX_2 (M is a transition metal and X is a chalcogen) sandwiches depending on coordination of the transition metal atom by the chalcogens.¹ In 1T-MX_2 the coordination is octahedral, whereas in 2H-MX_2 it is trigonal prismatic. The M - X bonds are strongly covalent, but the sandwich layers are coupled only by weak van der Waals (vdW) interactions, resulting in easy slippage as well as easy cleavage of planes.

Recently, a single layer of MoS_2 (1L- MoS_2 ; S-Mo-S), which is obtained by employing the microexfoliation technique as popularly used in order to produce a graphene,² has aroused much interest for its many remarkable properties. Most of these properties follow from that the 1L- MoS_2 is a direct gap semiconductor with a gap energy (E_g) of ~ 1.8 eV, whereas bulk MoS_2 is an indirect gap semiconductor with $E_g = \sim 1.3$ eV.^{3,4} This direct gap transition in the single-layer limit³⁻⁵ was also observed in WS_2 ^{6,7} and WSe_2 .⁸ More recently, theoretical studies have also revealed that indirect gap semiconductors 2H-MX_2 ($M = \text{Mo, W}$; $X = \text{S, Se, Te}$) become direct gap semiconductors with significantly larger E_g than those of the bulks when thinned to a single layer.^{9,10}

More surprisingly, the excellent current on/off ratios of 1×10^8 and ultralow standby power dissipation have been realized in the fabrication of a field-effect transistor based on a 1L- MoS_2 .¹¹ In fact, the mobilities of single layer or thin film of MoS_2 in the 0.1 – 10 cm^2/Vs range^{2,12} are too low to be applicable to practical devices. On the other hand, it has been revealed that deposition of thick HfO_2 (30 nm) on a 1L- MoS_2 dramatically enhances the mobilities in the ~ 200 cm^2/Vs range,¹¹ which is comparable to the value of bulk (200 – 500 cm^2/Vs).¹³ Although the reason of the reduced and recovered mobility of 1L- MoS_2 has been explained by

using the Coulomb scattering model,^{11,14} which is crucial in the graphene's transport properties,¹⁵ the conductivities of 1L- and few-layer MoS_2 show that the dependences on the gate voltage are roughly linear different from that of graphene^{2,12} and, therefore, other mechanisms need to be included for a complete understanding of how the mobility of bulk reduces upon lowering the numbers of layers and recovers the reduced mobility of 1L- MoS_2 by the deposition of high- κ dielectric. In this Brief Report, we find that the electronic structures of 2H-MX_2 strongly depend on the number of layers, and the strain has the significant influence on the single layer.

For the bulk and the film of 2H-MX_2 , we used full-potential linearized augmented plane wave (FLAPW) method^{16,17} to solve the density functional Kohn-Sham equations. The general gradient approximation (GGA)¹⁸ was adopted to describe the exchange-correlation potential. Energy cut-offs of 12.25 Ry and 256 Ry were employed for the basis expansion and the charge-potential within the interstitial region, respectively, and spherical harmonics with $l \leq 8$ inside the muffin-tin spheres. In the Brillouin zone 7296 and 470 k -points were used in summation for the bulk and film, respectively.

Since it has been suggested that the experimental lattice constants¹⁹⁻²¹ of bulk 2H-MX_2 well produce the band gap of single layer,^{22,23} we employed those in the present calculations, as listed in Table I. Subsequently, all atoms were allowed to be relaxed through a total energy minimization that was guided by the calculated atomic forces. The resultant z parameters, the distance (\AA) between the M layer and the X layer in a sandwich, are also given in Table I.

Effective masses of hole (m_h^*) and electron (m_e^*) of MoS_2 , the prototypical TMD of 2H-MX_2 , were derived at high-symmetry points and listed in Table II.

Figure 1 displays the gap transition of 2H-MX_2 upon reducing the numbers of layers from the bulk (upper panels) to the double-layer (middle panels) to the single-layer (bottom panels). Each of the bulk compounds shows an indirect gap consisting of a valence band maximum (VBM) at the Γ -point and a conduction band minimum (CBM) at a midpoint along Γ -K symmetry lines. As the number of layers reduces, both

TABLE I. Lattice parameters a and c of $2\text{H-}MX_2$ ($M = \text{Mo, W; } X = \text{S, Se, Te}$) (Refs. 20–22) and the internal coordinate z , which determines the intralayer chalcogen plane distance. The strain effects on $1\text{L-}MX_2$ [Fig. 3] retain the direct gap and metallic state in the range of lattice a .

	a (Å)	c (Å)	z_{bulk}	$z_{2\text{L}}$	$z_{1\text{L}}$	direct gap (% of a)	metal (% of a)
MoS ₂	3.160	12.296	1.565	1.572	1.572	−1.3 ~ 0.3	9.8
MoSe ₂	3.299	12.939	1.669	1.606	1.676	−0.9 ~ 2.5	11.5
MoTe ₂	3.522	13.968	1.809	1.816	1.815	−0.3 ~ 5	12.2
WS ₂	3.155	12.349	1.573	1.578	1.58	−0.2 ~ 0.5	10.9
WSe ₂	3.286	12.976	1.682	1.686	1.688	0 ~ 3.2	12.9

the VBM and the CBM move toward the K-point and direct band gaps are obtained at all the single layers, where there exists no noticeable vdW interlayer-interaction. Note that up to the triple layers (not shown) from the bulk, the indirect gap remains between the Γ -point of VBM and the midpoint of CBM with enhancing the gap energy.

Based on previous studies,^{5–10,23} the total density of states near the Fermi level originates from mostly TM d -states with weak contribution of chalcogen p -states. In detail, the VBM and CBM at K-point, which consist of a direct gap in the single layer, are predominantly derived from xy/x^2-y^2 and z^2 orbitals, respectively. On the other hand, the VBM near the Γ -point is derived from the z^2 orbitals and the CBM at a midpoint consists of the xz and yz orbitals.

The variations of E_g are summarized in Fig. 2. While the indirect band gap of bulk materials are in the range of near infrared, single layers are expected to be promising materials for the solar cells because the band gaps match well with the range of visible light as well as being a direct band gap. Especially, both the 1L- (1.47 eV) and 2L- (1.46 eV) MoSe₂ have optimum band gaps (1.3–1.5 eV) for solar energy conversion.^{24,25} It is also noticeable that 1L-MoS₂ and 1L-WS₂ have E_g within the optimum range (1.8–2.0 eV) for photoelectrochemical production of hydrogen from water.²⁶

Even though the indirect-to-direct gap transition of $2\text{H-}MX_2$ upon reducing the thickness to single layer has been revealed throughout recent first-principles calculations,^{9,10} we found some characteristic differences.

First of all, based on the increase of gap energy upon lowering the number of layers (see Fig. 2), the reason of the reduction of mobility^{2,12} in the single- or few-layer MoS₂ is mainly due to the decrease of carrier concentration, which is also contributed partly by the Coulomb scattering,¹⁵ near Fermi level with respect to that of bulk. Accordingly the limited

phonon scattering with decreasing the numbers of layers has been also revealed from the Raman spectroscopy²⁷ that the A_{1g} (out-plane) vibration frequency decreases dramatically, while the E_{12g}^1 (in-plane) vibration frequency increases slightly.²⁸ In addition, the effective masses vary, as given in Table II. From the bulk to 1L-MoS₂ (2L-MoS₂), the m_h^* at the Γ -point dramatically increases to $\sim 396\%$ ($\sim 64\%$), and the m_h^* at the K-point and the m_c^* at the midpoint just slightly increases, respectively. In total the increase of effective masses also elucidates why the mobility reduces upon lowering the numbers of layers. However, for the case of double and single layers, we need to consider carefully the change of lowest points. The change of CBM from the midpoint to the K-point may have no significant effect because of their similar effective masses. In contrast, the change of VBM from the Γ -point to the K-point, where the m_c^* for 1L-MoS₂ (2L-MoS₂) decreases to $\sim 41\%$ ($\sim 34\%$), induces the dramatic decrease of effective masses and the mobility should be increased. It is contrary to the experimental results.^{2,12} However, the consideration of carrier concentration may be helpful because it depends on not only the band gap energy, but also the effective masses,²⁹ i.e., the carrier concentration at the K-point would be lower than that at the Γ -point. We could also consider that the mobilities of charge carriers are mainly related to the Mo d_{z^2} electrons, which have the contribution to the VBM of Γ -point through the vdW-interlayer-interaction. On the other hand, the Mo d_{xy/x^2-y^2} electrons at the VBM of K-point have the negligible contribution to the mobility due to the strong covalent bonding. These dependences of carrier density and effective masses upon the variation of thickness well explain the reduced mobility of 1L-MoS₂ than the Coulomb scattering model.¹¹

We have also studied the influence of strain on the electronic structure of $1\text{L-}MX_2$. Figure 3(a) shows that even a just

TABLE II. Calculated the hole and electron effective masses (m^*) at the high symmetry points. The effective masses for the bulk, 2L-, and 1L-MoS₂ are derived from the band structures as shown in Fig. 1. The effective masses for the strain effects are derived from those as shown in Fig. 3. The unit is of the electron rest mass (m_e).

Symmetry Point	Fig. 1			Fig. 3		
	Bulk	2L	1L	(b) $a = 3.100$ Å	(c) $a = 3.299$ Å	
m_h^*/m_e	Γ	0.711	1.168	3.524	8.049	1.527
	K	0.625	0.628	0.637	0.703	0.594
m_c^*/m_e	midpoint	0.551	0.579	0.569	0.564	0.565
	Γ K	0.821	0.542	0.483	0.585	0.405

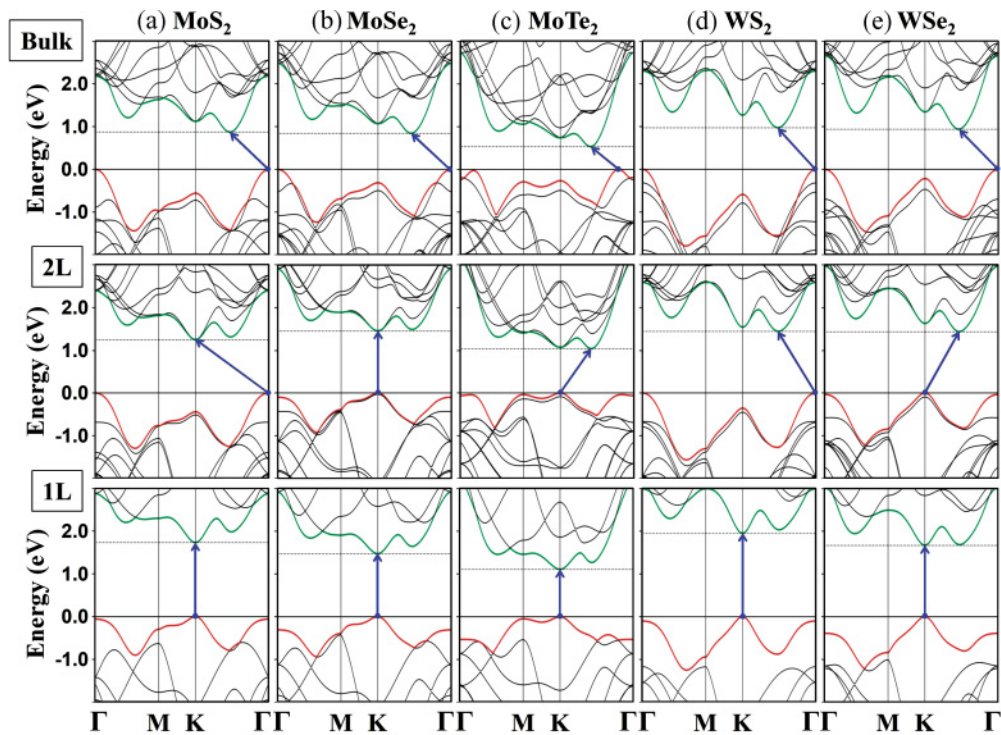


FIG. 1. (Color online) Band structures of (a) MoS₂, (b) MoSe₂, (c) MoTe₂, (d) WS₂, and (e) WSe₂ from the bulk (upper panels) to double-layer (2L, middle panels) and single-layer (1L, bottom panels). The horizontal solid lines in each panel indicate the VBM and the dotted lines indicate the CBM. The solid blue arrows indicate the lowest energy transitions.

slightly different lattice value for 1L-MoS₂ from the bulk optimum value of $a = 3.16 \text{ \AA}$ induces the direct-to-indirect gap transition with changing the gap energy and the positions of the VBM and CBM. The direct band gap is maintained only in a quite narrow range of -1.3 to 0.3% , deviated from the optimum value. Furthermore, the increased a more than

$\sim 9.8\%$ is found to become metallic. Upon the strain the other single layers also retain the direct gap and become metallic in the range of lattice a as given in Table I, respectively.

Figures 3(b), 3(c), and 3(d) correspond to the band structures of 1L-MoS₂ under compressive and tensile stresses on 1L-MoS₂, respectively. In Fig. 3(b) the reduced lattice constant

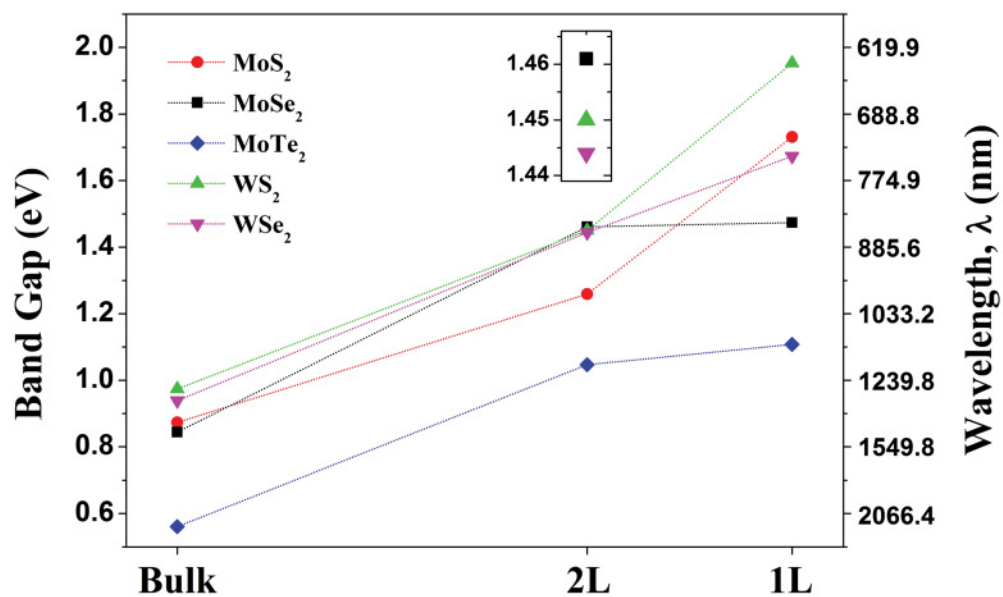


FIG. 2. (Color online) Thickness dependence of band gap energies of 2H- MX_2 ($M = \text{Mo, W; } X = \text{S, Se, Te}$). Right axis corresponds to the wavelengths.

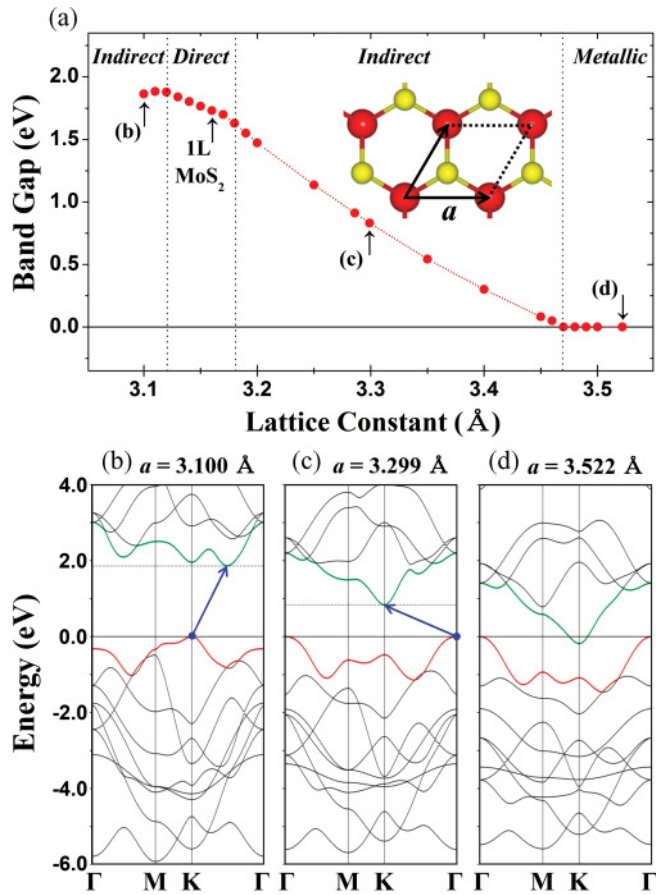


FIG. 3. (Color online) (a) Strain dependence of band gap energies of 1L-MoS₂ ($a = 3.160$ Å). The representative band structures for the (b) compressive and (c), (d) tensile stresses are displayed, respectively. Inset indicates the hexagonal structure consisting of Mo (red/gray balls) and S (yellow/light gray balls) from the top views.

of $a = 3.100$ Å (-1.9% , compressive stress) enhances E_g from 1.73 to 1.86 eV with changing the position of CBM to the midpoint from the K-point. Accordingly the m_h^* at the Γ - and K-points and the m_c^* at the K-point increase by $\sim 128\%$, $\sim 10\%$, and $\sim 21\%$ compared to those of the unstrained 1L-MoS₂, respectively. Notably, the compressive stress is supposed to reduce the mobility of 1L- MX_2 . However, we became aware of concurrent and independent work (only the case of MoS₂),³⁰ which reports that the excessive compression leads to be metallic.

In the case of tensile stress, the increased lattice of $a = 3.299$ Å (4% , tensile stress) as shown in Fig. 3(c) reduces the E_g to 0.83 eV. In further the tensile stress larger than 11% [Fig. 3(d)] leads to be metallic. The position of VBM is also changed from the K-point to the Γ -point while the CBM retains at the K-point. These results support the enhancement of carrier concentration. Accordingly the m_h^* at the Γ - and the K-point and the m_c^* at the K-point are also decreased to $\sim 57\%$, $\sim 7\%$, and $\sim 16\%$, compared to those of the unstrained 1L-MoS₂, respectively.

In comparison with the compressive stress, the tensile stress explains how the reduced mobility of 1L-MoS₂ recovers by deposition thick HfO₂.¹¹ Since 1L-MoS₂ has been revealed to be locally puckered³¹ as freely suspended or loosely adhered to a substrate, the deposition of high- κ dielectric materials is enough to form the lattice-mismatched strain. Much very recently, these predictions have been verified experimentally. The temperature dependent photoluminescence (PL) on 1L-MoS₂ shows that the band gap energy increases upon lowering temperature and furthermore the two PL peaks with the energy difference of 90 meV are observed.^{32,33} These results are similar with the compressive strain induced direct-to-indirect gap transition with increasing the band gap energy. The two peaks at low temperatures would be related to the coexistence of direct and indirect band gaps such as the case of 2L-MoS₂.⁴ In addition, the oxide-covered-flakes confirm the strain effects on 1L-MoS₂, i.e., the Al₂O₃ and HfO₂ increases and decreases the band gap energy, respectively. The former and latter correspond to the compressive and tensile strains, respectively. These experimental evidences are in best agreement with our findings.³³

In conclusion, we have revealed that the electronic band structures of 2H- MX_2 ($M = \text{Mo, W}$; $X = \text{S, Se, Te}$) semiconductors are strongly dependent on the numbers of layers and the strain (lattice constants). All bulk MX_2 with an indirect gap has been confirmed to be a direct gap in the single layer with the limit of lattice constants. Our findings on the 1L- MX_2 such as the increase of band gap with a transition to the direct gap, the change of band curvatures, i.e., the increase of effective masses and the strain effects explain how the mobility reduces and recovers, respectively.

ACKNOWLEDGMENTS

This Brief Report was supported by the Basic Research Program (Grant No. 2010-0008842), and the Priority Research Centers Program (Grant No. 2009-0093818) through the NRF funded by MEST.

*Corresponding author: swan72@ulsan.ac.kr

†Corresponding author: schong@ulsan.ac.kr

¹J. A. Wilson and A. D. Yoffe, *Adv. Phys.* **18**, 193 (1969).

²K. S. Novoselov, D. Jiang, F. Schedin, T. Booth, V. V. Khotkevich, S. V. Morozov, and A. K. Geim, *Proc. Natl. Acad. Sci. USA* **102**, 10451 (2005).

³A. Splendiani, L. Sun, Y. Zhang, T. Li, J. Kim, C.-Y. Chim, G. Galli, and F. Wang, *Nano Lett.* **10**, 1271 (2010).

⁴K. F. Mak, C. Lee, J. Hone, J. Shan, and T. F. Heinz, *Phys. Rev. Lett.* **105**, 136805 (2010).

⁵T. Li and G. Galli, *J. Phys. Chem. C* **111**, 16192 (2007).

⁶A. Klein, S. Tiefenbacher, V. Eyert, C. Pettenkofer, and W. Jaegermann, *Phys. Rev. B* **64**, 205416 (2001).

- ⁷K. Albe and A. Klein, *Phys. Rev. B* **66**, 073413 (2002).
- ⁸D. Voß, P. Krüger, A. Mazur, and J. Pollmann, *Phys. Rev. B* **60**, 14311 (1999).
- ⁹Y. Ding, Y. Wang, J. Ni, L. Shi, S. Shi, and W. Tang, *Physica B* **406**, 2254 (2011).
- ¹⁰A. Kuc, N. Zibouche, and T. Heine, *Phys. Rev. B* **83**, 245213 (2011).
- ¹¹B. Radisavljevic, A. Radenovic, J. Brivio, V. Giacometti, and A. Kis, *Nat. Nanotechnol.* **6**, 147 (2011).
- ¹²A. Ayari, E. Cobas, O. Ogundadegbe, and M. S. Fuhrer, *J. Appl. Phys.* **101**, 014507 (2007).
- ¹³R. Fivaz and E. Mooser, *Phys. Rev.* **163**, 743 (1967).
- ¹⁴D. Jena and A. Konar, *Phys. Rev. Lett.* **98**, 136805 (2007).
- ¹⁵Y.-W. Tan, Y. Zhang, K. Bolotin, Y. Zhao, S. Adam, E. H. Hwang, S. Das Sarma, H. L. Stormer, and P. Kim, *Phys. Rev. Lett.* **99**, 246803 (2007).
- ¹⁶E. Wimmer, H. Krakauer, M. Weinert, and A. J. Freeman, *Phys. Rev. B* **24**, 864 (1981).
- ¹⁷M. Weinert, E. Wimmer, and A. J. Freeman, *Phys. Rev. B* **26**, 4571 (1982).
- ¹⁸J. P. Perdew, K. Burke, and M. Ernzerhof, *Phys. Rev. Lett.* **77**, 3865 (1996).
- ¹⁹J. C. Wildervanck and F. Jellinek, *Z. Anorg. Allgem. Chem.* **328**, 309 (1964).
- ²⁰A. A. Al-Hilli and B. L. Evans, *J. Cryst. Growth* **15**, 93 (1972).
- ²¹R. Manzke and M. Skibowski in: *Electronic Structure of Solids: Photoemission Spectra and Related Data, Landolt Börnstein*, edited by A. Goldmann (Springer-Verlag, Berlin, 1994), Chap. 2.7.3 VIB-VIA-compounds.
- ²²L. Liu, S. B. Kumar, Y. Ouyang, and J. Guo, *IEEE Trans. Electron Devices* **58**, 3042 (2011).
- ²³S. W. Han, H. Kwon, S. K. Kim, S. Ryu, W. S. Yun, D. H. Kim, J. H. Hwang, J.-S. Kang, J. Baik, H. J. Shin, and S. C. Hong, *Phys. Rev. B* **84**, 045409 (2011).
- ²⁴J. J. Loferski, *J. Appl. Phys.* **27**, 777 (1956).
- ²⁵MoSe₂ becomes a direct gap semiconductor even in the double-layers while the three layers are still indirect gap. This may be related to the unusual change of the vdW gap and layer thickness. However, the Vienna *ab initio* simulation package (VASP) calculation results in the indirect gap of 2L-MoSe₂. It needs to be elucidated from the experimental measurement.
- ²⁶J. Nowotny, C. C. Sorrel, L. R. Sheppard, and T. Bak, *Int. J. Hydrogen Energy* **30**, 521 (2005).
- ²⁷C. Lee, H. Yan, L. E. Brus, T. F. Heinz, J. Hone, and S. Ryu, *ACS Nano* **4**, 2695 (2010).
- ²⁸A. Molina-Sánchez and L. Wirtz, *Phys. Rev. B* **84**, 155413 (2011).
- ²⁹C. Kittel, *Introduction to Solid State Physics*, 8th Ed. (Wiley, New York, 2005) p. 206.
- ³⁰E. Scalise, M. Houssa, G. Pourtois, V. Afanas'ev, and A. Stesmans, *Nano Research* **5**, 43 (2012).
- ³¹C. Lee, Q. Li, W. Kalb, X.-Z. Liu, H. Berger, R. W. Carpick, and J. Hone, *Science* **328**, 76 (2010).
- ³²T. Korn, S. Heydrich, M. Hirmer, J. Schmutzler, and C. Schüller, *Appl. Phys. Lett.* **99**, 102109 (2011).
- ³³G. Plechinger, F.-X. Schrettenbrunner, J. Eroms, D. Weiss, C. Schüller, and T. Korn, eprint [arXiv:1112.3747](https://arxiv.org/abs/1112.3747) (2011).